ELSEVIER

0263-8223(95)00069-0

Composite Structures **32** (1995) 583–591

0263-8223/95/$9.50

First-ply failure analysis of laminated composite plates based on the layerwise linear displacement theory

T. Y. Kam & T. B. Jan

Department of Mechanical Engineering, National Chiao Tung University, Hsin-Chu 30050, Taiwan, ROC

A finite element formulated on the basis of the layerwise linear displacement theory is used to study the first-ply failure of moderately thick laminated composite plates. In the finite element formulation, a laminated composite element is divided into a number of mathematical layer groups and displacements are assumed to vary linearly in each layer group which contains eight nodal points. The accuracy of the finite element in predicting displacements and stresses has been verified by comparing results with experimental data and previously obtained analytical results. The finite element is used to determine the first-ply failure loads of a number of laminated composite plates on the basis of several phenomenological failure criteria. The capabilities of the failure criteria in predicting first-ply failure loads are investigated by comparing the finite element first-ply failure loads with the experimental ones. It has been found that the failure criteria can yield reasonably good results for the cases considered.

1 INTRODUCTION

Due to their high stiffness/strength to weight ratios and long fatigue life, laminated composite materials have recently found extensive applications in the construction of mechanical, aerospace, marine and automotive structures which, in general, require high reliability. For reliability assurance, the predictions of the failure process of laminated composite structures and the maximum loads that the structures can withstand before failure occurs have thus become an important topic of research. In particular, the first-ply failure analysis of laminated composite plates subjected to transverse loads has drawn close attention in recent years.[1–9] For example, Turvey[1–4] used analytical methods to study the linear and nonlinear first-ply failure loads of simply supported symmetrically and antisymmetrically laminated composite plates based on the classical lamination theory; Reddy and his associates[5,6] used the finite element method which is formulated on the basis of the first order shear deformation theory to calculate the linear and nonlinear first-ply failure loads of laminated composite plates based on several phenomenological failure criteria; Kam and his associates[7–10] studied the first-ply failure loads, first-ply failure probabilities and ultimate loads of linear and nonlinear laminated composite plates. Most of the previous works, however, have been concentrated on first-ply failure analysis of thin laminates under transverse loads. Not much work on failure of moderately thick laminates has been reported in the literature. In this paper, a finite element formulated on the basis of the layerwise linear displacement theory is presented for studying the deformation and first-ply failure of thick laminated composite plates. The accuracy of the proposed finite element method is validated via the comparison of the present finite element results with those reported in the literature. Its ability in predicting first-ply failure loads of laminated composite plates is studied using experimental data.

2 LAYERWISE LINEAR DISPLACEMENT THEORY

The laminated composite plate under consideration is made of a number of orthotropic layers of equal thickness. The x and y coor-

dinates of the plate are taken in the midplane of the plate which has area $a \times b$ and thickness h. In the plate analysis, the thickness of the laminated composite plate in Fig. 1a is divided into a number of mathematical layer groups in which the displacement components of each layer group are assumed to vary linearly.

(i) Displacement in x-direction

$$u_1 = u_0 + \xi_1 \psi_{x1}$$

and

$$u_i = u_0 + \frac{t_1}{2}\psi_{x1} + \sum_{k=2,4,}^{i-2} t_k \psi_{xk} + \xi_i \psi_{xi} \quad (i = 2, 4, 6, \ldots, NL-1) \tag{1}$$

$$u_i = u_0 - \frac{t_1}{2}\psi_{x1} - \sum_{k=3,5,}^{i-2} t_k \psi_{xk} + \xi_i \psi_{xi} \quad (i = 3, 5, 7, \ldots, NL)$$

(ii) Displacement in y-direction

$$v_1 = v_0 + \xi_1 \psi_{y1}$$

and

$$v_i = v_0 + \frac{t_1}{2}\psi_{y1} + \sum_{k=2,4,}^{i-2} t_k \psi_{yk} + \xi_i \psi_{yi} \quad (i = 2, 4, 6, \ldots, NL-1) \tag{2}$$

$$v_i = v_0 - \frac{t_1}{2}\psi_{y1} - \sum_{k=3,5,}^{i-2} t_k \psi_{yk} + \xi_i \psi_{yi} \quad (i = 3, 5, 7, \ldots, NL)$$

(iii) Displacement in z-direction

$$w_1 = w_0 + \xi_1 \psi_{z1}$$

and

$$w_i = w_0 + \frac{t_1}{2}\psi_{z1} + \sum_{k=2,4,}^{i-2} t_k \psi_{zk} + \xi_i \psi_{zi} \quad (i = 2, 4, 6, \ldots, NL-1) \tag{3}$$

$$w_i = w_0 - \frac{t_1}{2}\psi_{z1} - \sum_{k=3,5,}^{i-2} t_k \psi_{zk} + \xi_i \psi_{zi} \quad (i = 3, 5, 7, \ldots, NL)$$

where ξ_i is the local coordinate for the ith layer group; u_i, v_i, w_i are displacement components in the x, y, z directions, respectively, for the ith layer group; u_0, v_0, w_0 are the displacements in the mid-plane; ψ_{xi}, ψ_{yi}, ψ_{zi} are rotational degrees of freedom of the ith layer group; NL is number of layer groups; t_i is the thickness of the ith layer group. It is noted that no summation is performed in the above equations if $(i-2)$ is less than k. Figure 2 shows the displacements of the layer groups across plate thickness in the x-direction.

The constitutive relations of a lamina with fiber angle θ are expressed as

$$\begin{bmatrix} \sigma_x \\ \sigma_y \\ \sigma_z \\ \tau_{yz} \\ \tau_{xz} \\ \tau_{xy} \end{bmatrix} = \begin{bmatrix} \bar{Q}_{11} & \bar{Q}_{12} & \bar{Q}_{13} & 0 & 0 & \bar{Q}_{16} \\ \bar{Q}_{21} & \bar{Q}_{22} & \bar{Q}_{23} & 0 & 0 & \bar{Q}_{26} \\ \bar{Q}_{13} & \bar{Q}_{23} & \bar{Q}_{33} & 0 & 0 & \bar{Q}_{36} \\ 0 & 0 & 0 & \bar{Q}_{44} & \bar{Q}_{45} & 0 \\ 0 & 0 & 0 & \bar{Q}_{45} & \bar{Q}_{55} & 0 \\ \bar{Q}_{16} & \bar{Q}_{26} & \bar{Q}_{36} & 0 & 0 & \bar{Q}_{66} \end{bmatrix} \cdot \begin{bmatrix} \varepsilon_x \\ \varepsilon_y \\ \varepsilon_z \\ \gamma_{yz} \\ \gamma_{xz} \\ \gamma_{xy} \end{bmatrix} \tag{4}$$

where $\sigma_x, \ldots, \tau_{xy}$ are stress components; $\varepsilon_x, \ldots, \gamma_{xy}$ are strain components; $\bar{Q}_{ij}$ are material stiffness coefficients in the reference coordinate system. Expressions for evaluating $\bar{Q}_{ij}$ can be found in Ref. 11. Based on the linear elasticity theory, the strain-displacement relations are expressed as

$$\varepsilon_x = \frac{\partial u}{\partial x}, \quad \varepsilon_y = \frac{\partial v}{\partial y}, \quad \varepsilon_z = \frac{\partial w}{\partial z}$$

$$\gamma_{yz} = \frac{\partial v}{\partial z} + \frac{\partial w}{\partial y}, \quad \gamma_{xz} = \frac{\partial u}{\partial z} + \frac{\partial w}{\partial x}$$

$$\gamma_{xy} = \frac{\partial u}{\partial y} + \frac{\partial v}{\partial x} \tag{5}$$

The strain in each layer group can be obtained by substituting eqns (1)–(3) into eqn (5). For instance, strains in an even number layer group are written as:

$$\varepsilon_{x_i} = \frac{\partial u_0}{\partial x} + \frac{t_1}{2}\frac{\partial \psi_{x1}}{\partial x} + \sum_{k=2,4}^{i-2} t_k \frac{\partial \psi_{xk}}{\partial x} + \xi_i \frac{\partial \psi_{xi}}{\partial x}$$

$$\varepsilon_{y_i} = \frac{\partial v_0}{\partial y} + \frac{t_1}{2}\frac{\partial \psi_{y1}}{\partial y} + \sum_{k=2,4}^{i-2} t_k \frac{\partial \psi_{yk}}{\partial y} + \xi_i \frac{\partial \psi_{yi}}{\partial y}$$

$$\varepsilon_{z_i} = \psi_{zi}$$

$$\gamma_{yz_i} = \psi_{yi} + \frac{\partial w_0}{\partial y} + \frac{t_1}{2}\frac{\partial \psi_{z1}}{\partial y} + \sum_{k=2,4,}^{i-2} t_k \frac{\partial \psi_{zk}}{\partial y} + \xi_i \frac{\partial \psi_{zi}}{\partial y} \tag{6}$$

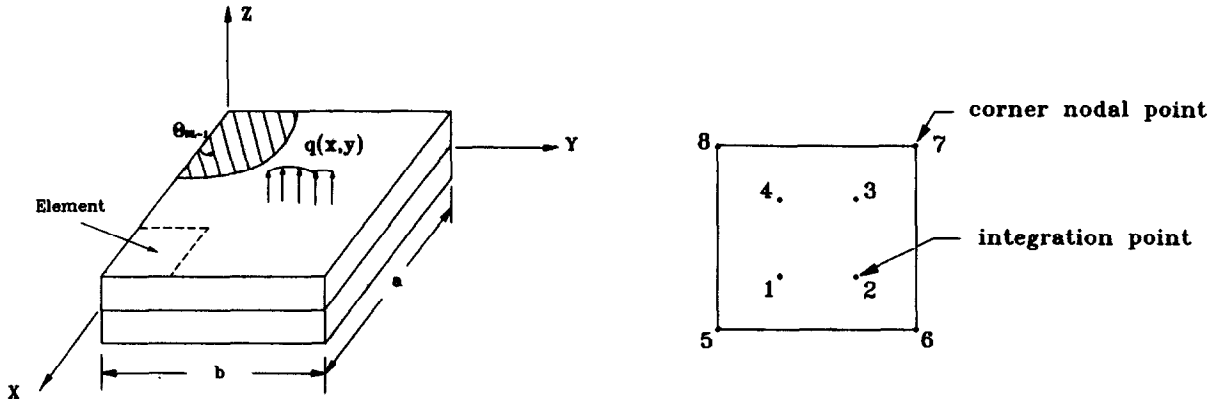

(a) Laminated plate

(b) Integration points in a layer group of an element

Fig. 1. Geometry and loading conditions of a laminated composite plate.

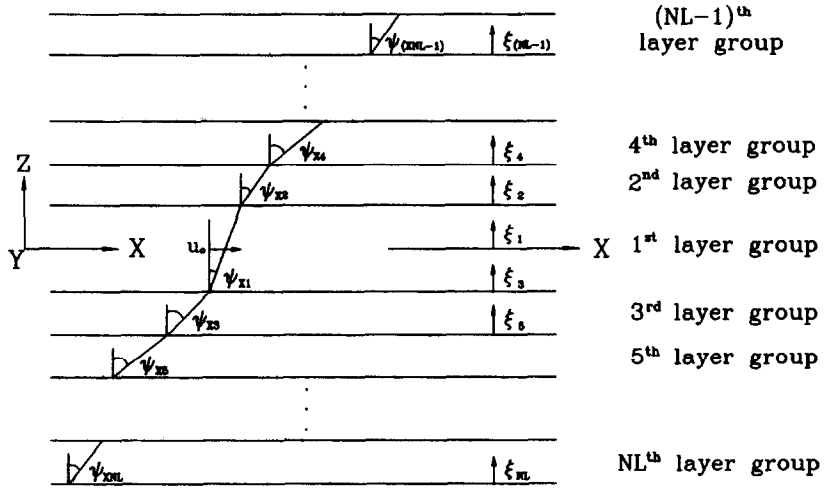

Fig. 2. Layerwise displacement components and local coordinates of layer groups.

$$\gamma_{xz_i} = \psi_{xi} + \frac{\partial w_0}{\partial x} + \frac{t_1}{2}\frac{\partial \psi_{z1}}{\partial x} + \sum_{k=2,4,}^{i-2} t_k \frac{\partial \psi_{zk}}{\partial x} + \xi_i \frac{\partial \psi_{zi}}{\partial x}$$

$$\gamma_{xy_i} = \frac{\partial u_0}{\partial y} + \frac{\partial v_0}{\partial x} + \frac{t_1}{2}\left(\frac{\partial \psi_{x1}}{\partial y} + \frac{\partial \psi_{y1}}{\partial x}\right) + \sum_{k=2,4,}^{i-2} t_k \left(\frac{\partial \psi_{xk}}{\partial y} + \frac{\partial \psi_{yk}}{\partial x}\right) + \xi_i \left(\frac{\partial \psi_{xi}}{\partial y} + \frac{\partial \psi_{yi}}{\partial x}\right)$$

$$(i = 2, 4, 6, \ldots, NL-1)$$

Similarly, no summation is performed in the above equation if $(i-2)$ is less than k.

3 FINITE ELEMENT FORMULATION

In the finite element formulation, the plate is discretized into a number of elements which are connected together via the nodes at the layer groups of the elements. The displacements at any point in each layer group are obtained via interpolation based on the layer nodal displacements and appropriate shape functions.

$$u_0 = N\bar{u} \quad v_0 = N\bar{v} \quad w_0 = N\bar{w}$$
$$\psi_{xi} = N\bar{\psi}_{xi} \quad \psi_{yi} = N\bar{\psi}_{yi} \tag{7}$$

where N is a $1 \times ND$ shape function vector; $\overline{(.)}$ denotes layer group nodal displacement vector;

ND is number of layer group nodes. Herein, a quadratic (*ND* = 8) formulation of the serendipity family with reduced integration of 2×2 Gauss rule is used for each layer group in constructing the element stiffness matrix. In view of eqns (4), (6) and (7), the load-displacement equations of the laminated plate are obtained via the standard finite element procedure as

$$\mathbf{K}\mathbf{V} = \mathbf{P} \tag{8}$$

K, **V**, **P** are structural stiffness matrix, nodal displacement vector, and nodal force vector, respectively. In the stress analysis, the stresses at the four corner nodes in Fig. 1b are obtained from those at the integration points using the following extrapolation equations,

$$\begin{aligned}\sigma_{i+5} &= \left(1+\frac{\sqrt{3}}{2}\right)\sigma_{i+1}+\left(1-\frac{\sqrt{3}}{2}\right)\sigma_{3-i} \\ &\quad -0{\cdot}5(\sigma_2+\sigma_4) \quad i=0,2 \\ \sigma_{i+6} &= \left(1+\frac{\sqrt{3}}{2}\right)\sigma_{i+2}+\left(1-\frac{\sqrt{3}}{2}\right)\sigma_{4-i} \\ &\quad -0{\cdot}5(\sigma_1+\sigma_3) \quad i=0,2\end{aligned} \tag{9}$$

where σ_i ($i = 1, \ldots, 4$) are stresses at integration points; σ_i ($i = 5, \ldots, 8$) are the corresponding stresses at the corner points. It is noted that the stress components in the thickness (z) directions obtained by the present finite element model do not satisfy equilibrium conditions at the interfaces between layer groups. To remedy this shortcoming, the plate thickness is divided into several regions and each region contains a number of layer groups. In each region the stress components in the z-direction are approximated by the following cubic equation,

$$\sigma_{iz}(x, y, z) = a_0 + a_1 z + a_2 z^2 + a_3 z^3 \quad i = x, y, z \tag{10}$$

The constants a_i ($i = 0, \ldots, 3$) are determined by the use of the least squares method with the observation of the stress boundary conditions at the top and bottom surfaces of the plate and the stress continuity conditions at the boundary of two neighbouring regions. The stresses obtained in the finite element analysis are then used to study the first-ply failure of the laminated plate. The load that makes the first-ply fail will be calculated based on five different failure criteria.[5]

(i) Maximum stress criterion (Independent)

The maximum stress criterion states that the stresses in the principal material directions must be less than the respective strengths, otherwise fracture is said to have occurred, that is,

$$\begin{aligned}&\sigma_1 < X_T; \quad \sigma_3 < Z_T; \quad \sigma_5 < S \\ &\sigma_2 < Y_T; \quad \sigma_4 < R; \quad \sigma_6 < S\end{aligned} \tag{11}$$

where σ_1, σ_2, σ_3 are normal stress components, σ_4, σ_5, σ_6 are shear stress components, X_T, Y_T, Z_T are the lamina normal strengths in the 1, 2, 3 directions and R, S are the shear strengths in the 23 and 12 planes, respectively. When σ_1, σ_2, σ_3 are of a compressive nature they should be compared with X_C, Y_C, Z_C which are normal strengths in compression along the 1, 2, 3 directions, respectively.

(ii) Maximum stress criterion (Polynomial)

The polynomial type maximum stress criterion can be expressed as

$$\begin{aligned}&(\sigma_1 - X_T)(\sigma_1 + X_C)(\sigma_2 - Y_T)(\sigma_2 + Y_C)(\sigma_3 - Z_T) \\ &\quad \times (\sigma_3 + Z_C)(\sigma_4 - R)(\sigma_4 + R)(\sigma_5 - S)(\sigma_5 + S) \\ &\quad \times (\sigma_6 - S)(\sigma_6 + S) = 0\end{aligned} \tag{12}$$

(iii) The Hoffman's criterion

The Hoffman's criterion can be expressed as

$$\begin{aligned}&\frac{1}{2}\left(-\frac{1}{X_T X_C}+\frac{1}{Y_T Y_C}+\frac{1}{Z_T Z_C}\right)(\sigma_2-\sigma_3)^2 \\ &\quad +\frac{1}{2}\left(\frac{1}{X_T X_C}-\frac{1}{Y_T Y_C}+\frac{1}{Z_T Z_C}\right)(\sigma_3-\sigma_1)^2 \\ &\quad +\frac{1}{2}\left(\frac{1}{X_T X_C}+\frac{1}{Y_T Y_C}-\frac{1}{Z_T Z_C}\right)(\sigma_1-\sigma_2)^2 \\ &\quad +\left(\frac{1}{X_T}-\frac{1}{X_C}\right)\sigma_1+\left(\frac{1}{Y_T}-\frac{1}{Y_C}\right)\sigma_2 \\ &\quad +\left(\frac{1}{Z_T}-\frac{1}{Z_C}\right)\sigma_3+\left(\frac{\sigma_4}{R}\right)^2+\left(\frac{\sigma_5}{S}\right)^2 \\ &\quad +\left(\frac{\sigma_6}{S}\right)^2 \geq 1\end{aligned} \tag{13}$$

(iv) The Tsai-Hill criterion

The Tsai-Hill criterion can be expressed as

Table 1. Material properties of composite materials

Material constants			Strength		
	Material I	Material II		Material I	Material II
E_1	25×10^6 psi	142·50 Gpa	X_T		2193·5 Mpa
E_2	10^6 psi	9·79 Gpa	X_C		2457·0 Mpa
E_3	10^6 psi	9·79 Gpa	$Y_T = Z_T$		41·3 Mpa
$G_{12} = G_{13}$	$0{\cdot}5 \times 10^6$ psi	4·72 Gpa	$Y_C = Z_C$	—	206·8 Mpa
G_{23}	$0{\cdot}5 \times 10^6$ psi	1·192 Gpa	R		61·28 Mpa
$v_{12} = v_{13}$	0·25	0·27	$S = T$		78·78 Mpa
v_{23}	0·25	0·25			

$$\left(\frac{\sigma_1}{X}\right)^2+\left(\frac{\sigma_2}{Y}\right)^2+\left(\frac{\sigma_3}{Z}\right)^2$$

$$-\left(\frac{1}{X^2}+\frac{1}{Y^2}-\frac{1}{Z^2}\right)^2\sigma_1\sigma_2$$

$$-\left(-\frac{1}{X^2}+\frac{1}{Y^2}+\frac{1}{Z^2}\right)^2\sigma_2\sigma_3$$

$$-\left(\frac{1}{X^2}-\frac{1}{Y^2}+\frac{1}{Z^2}\right)\sigma_1\sigma_3$$

$$+\left(\frac{\sigma_4}{R}\right)^2+\left(\frac{\sigma_5}{S}\right)^2+\left(\frac{\sigma_6}{S}\right)^2\geq 1 \qquad (14)$$

The values of X, Y, Z are taken as either X_T, Y_T and Z_T or as X_C, Y_C and Z_C depending upon the sign of σ_1, σ_2 and σ_3, respectively.

(v) Tsai-Wu criterion

The Tsai-Wu criterion can be expressed as

$$F_i\sigma_i+F_{ij}\sigma_i\sigma_j\geq 1 \qquad (15)$$

where

$$F_1=\frac{1}{X_T}-\frac{1}{X_C};\quad F_2=\frac{1}{Y_T}-\frac{1}{Y_C};$$

$$F_3=\frac{1}{Z_T}-\frac{1}{Z_C} \qquad (16)$$

$$F_{11}=\frac{1}{X_TX_C};\quad F_{22}=\frac{1}{Y_TY_C};\quad F_{33}=\frac{1}{Z_TZ_C}$$

$$F_{44}=\frac{1}{R^2};\quad F_{55}=\frac{1}{S^2};\quad F_{66}=\frac{1}{S^2}$$

$$F_{12}=-\frac{1}{2\sqrt{X_TX_CY_TY_C}};$$

Table 2. Properties of laminated plates and load applicator

Plate	Values
Length a	100 mm
Ply thickness h_i	0·155 mm
Lamination	$[0^\circ_4/90^\circ_4]_s$, $[0^\circ_8/90^\circ_8]_s$
Load applicator radius r	5·0 mm

$$F_{13}=-\frac{1}{2\sqrt{X_TX_CZ_TZ_C}};$$

$$F_{23}=-\frac{1}{2\sqrt{Y_TY_CZ_TZ_C}}$$

4 EXPERIMENTAL INVESTIGATION

To verify the validity and accuracy of the proposed finite element, several centrally loaded laminated composite square plates of various lamination arrangements and side-to-thickness ratios were tested to failure. The laminated composite plates were made of graphite/epoxy (Q-1115) prepreg tapes supplied by Toho Co., Japan, with the material properties (Material II) determined experimentally and given in Table 1. The experimental apparatus consists of a 10-ton Instron testing machine, an acoustic emission (AE) system (AMS3), a linear vertical displacement transducer (LVDT), a data acquisition system, a steel load applicator with a spherical head, and a fixture for clamping the specimens. The dimensions of the laminated plates and the load applicator are given in Table 2. The fixture was made up of two steel frames which were connected together by four bolts. A stroke control approach was adopted in constructing the load-deflection relations for the laminated plates. The loading rate was slow enough for inertia effects to be neglected. Dur-

Table 3. Nondimensional deflections and stresses of $[0°/90°]_s$ plate under transverse sinusoidal load

a/h	Source	$\bar{W}$	$\bar{\sigma}_x$	$\bar{\sigma}_y$	$\bar{\tau}_{xy}$
10	Pagano & Hatfield[12]	1·709	0·559	0·403	0·0276
	Present (3 layers)	1·685	0·561	0·405	0·0277
	Reddy FEM[13]*	1·534	0·484	0·350	0·0234
	Panda & Natarajan[14]	1·448	0·532	0·307	0·0250
	Mawenya & Davies[15]	2·034	0·542	—	0·0292
20	Pagano & Hatfield[12]	1·189	0·543	0·309	0·0230
	Present (3 layers)	1·182	0·554	0·316	0·0234
	Reddy FEM[13]*	1·136	0·511	0·287	0·0214
	Panda & Natarajan[14]	1·114	0·557	0·307	0·0231
	Mawenya & Davies[15]	1·273	0·546	—	0·0239

$$\bar{w} = \frac{\alpha h^3 W}{p_0 a^4}, \quad \bar{\sigma} = \frac{h^2 \sigma}{p_0 a^2}, \quad \bar{\tau} = \frac{h^2 \tau}{p_0 a^2}$$

$$\alpha = \frac{\{4G_{12} + [E_1 + (1+2\nu_{12})E_2]/(1-\nu_{12}\nu_{21})\}\pi^4}{12}$$

*: Evaluated at Gauss point.

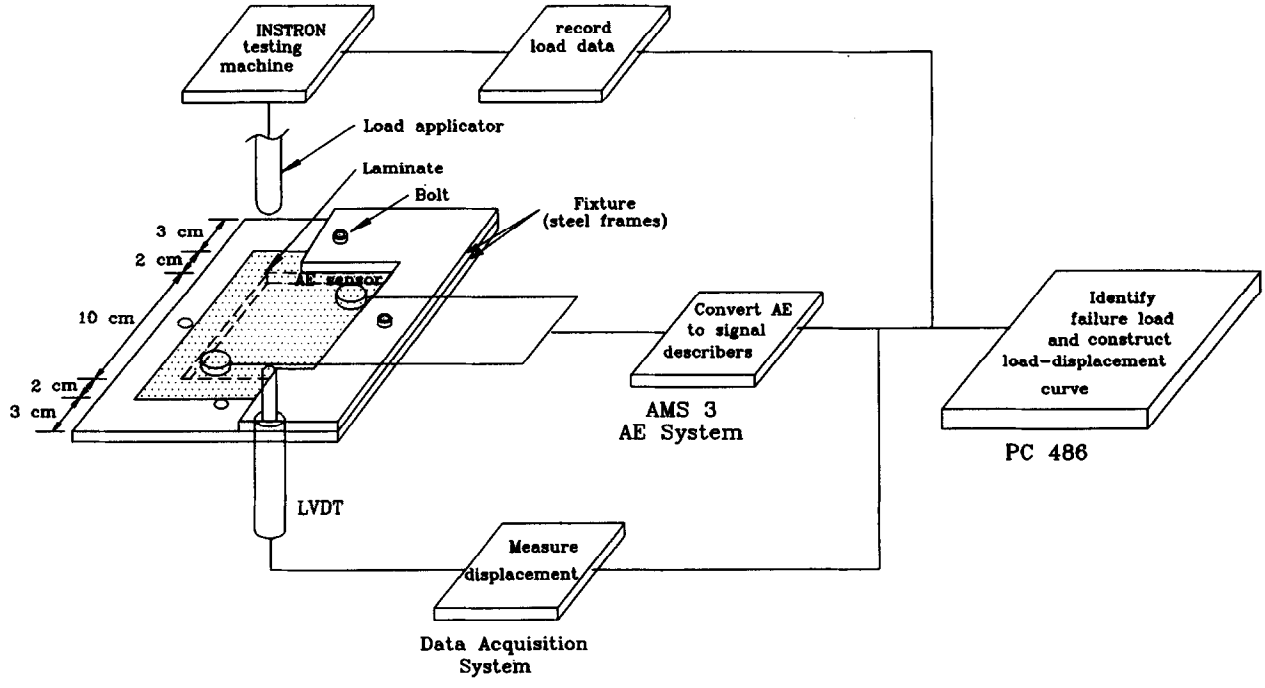

Fig. 3. A schematic description of the experimental setup.

ing loading, the LVDT displacement gage and data acquisition system were used to measure deflection data and construct the load-displacement curve of the laminated plate under testing. In addition, two acoustic emission sensors were used to measure the stress waves released at the AE sources in the laminated plate. The measured acoustic emissions were converted by the AMS3 (AE) system to a set of signal describers such as peak amplitude, energy, rise time and duration which were then used to identify the first-ply failure load of the laminated plate. A schematic description of the experimental procedure is shown in Fig. 3. As an example, Fig. 4 shows the load-displacement curve obtained from experiment and Fig. 5 the load-energy relations derived from the AE system for the $[0_8°/90_8°]_s$ plate.

5 RESULTS AND DISCUSSION

The accuracy of the proposed finite element in predicting displacements and stresses is first

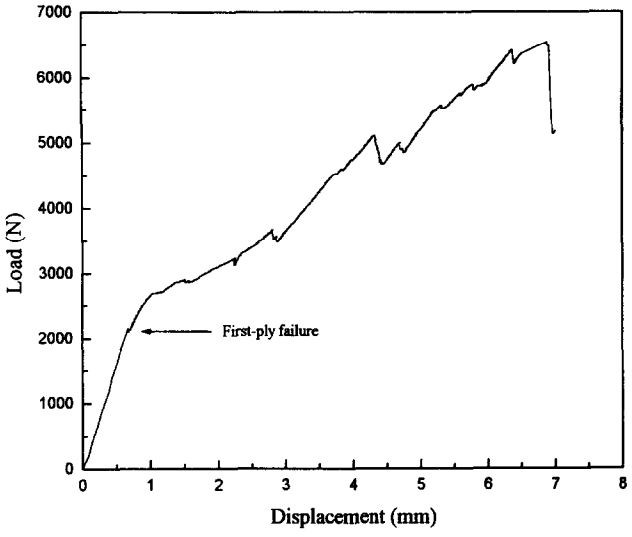

Fig. 4. Load-displacement curve of the $[0_8^\circ/90_8^\circ]_s$ plate.

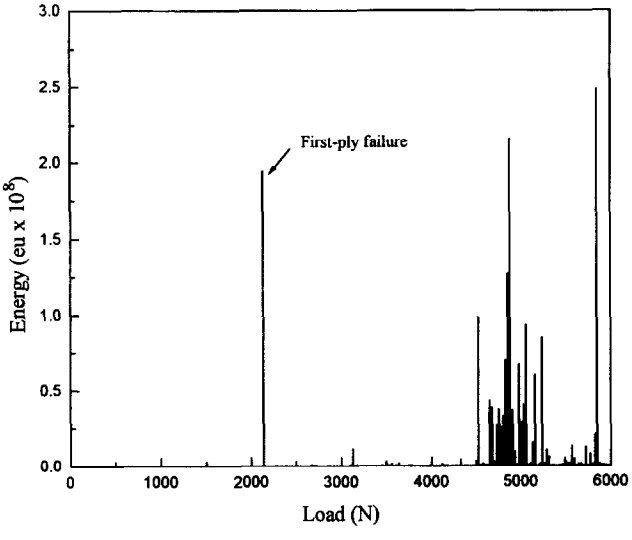

Fig. 5. Load-energy relations derived from AE system for the $[0_8^\circ/90_8^\circ]_s$ plate.

studied by comparing results with experimental data or analytical results reported in the literature. The static analysis of a simply supported $[0°/90°]_s$ square plate of material I under sinusoidal transverse load is performed. The results for length-to-thickness ratio $a/h = 10$ and 20 using 4×4 mesh for a quarter of the plate and three layer groups are listed in Table 3 in comparison with the results obtained by other researchers. It is noted that the stresses obtained by the present method are in good agreement with those obtained by the elasticity solution.[12] Furthermore, the continuous distribution of transverse shear stress τ_{xz} obtained by the present method using five layer groups for a simply supported [0°/90°/0°] square plate of $a/h = 4$ and material I in Fig. 6 illustrates the

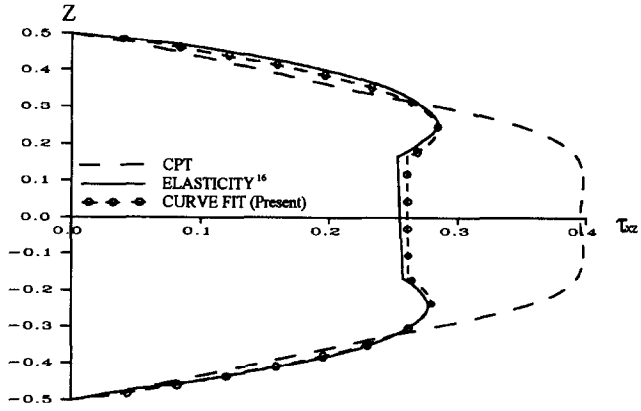

Fig. 6. Distribution of transverse shear stress τ_{xz} for [0°/90°/0°] plate subject to sinusoidal load.

feasibility and accuracy of the present method. A 32-layer $[0_8^\circ/90_8^\circ]_s$ plate of material II was tested and the load-displacement curve has been shown in Fig. 4. The center displacement of the plate under 1000 N was measured as 0·24 mm. Using this present finite element method with 4×4 mesh for a quarter of the plate and three layer groups, the displacement is computed as 0·212 mm which gives an error of 11·6% when compared with the experimental results.

Based on several phenomenological failure criteria, the present finite element is used to predict the first-ply failure loads of 16-layer $[0_4^\circ/90_4^\circ]_s$ and 32-layer $[0_8^\circ/90_8^\circ]_s$ plates whose actual first-ply failure loads have been determined experimentally from the mean value of 4 specimens for each type of lamination scheme via the AE system. For comparison purpose, the first-ply failure loads of the plates are also computed using the finite element constructed on the basis of the Mindlin plate theory.[17] The analytical and experimental results are listed in Tables 4 and 5 for comparison. It is noted that the present finite element method coupled with the failure criteria can yield very good results when compared with the experimental ones.

6 CONCLUSION

A laminated composite material finite element formulated on the basis of the layerwise linear displacement theory was presented. The accuracy of the finite element was verified by the experimental data obtained in this study and analytical results available in the literature. The finite element was used to study the first-ply failure load of moderately thick laminated

Table 4. Experimental and analytical first-ply failure loads of the $[0^\circ_4/90^\circ_4]_s$ plate

A. Experimental (N)	B. Analytical (N)				
	Failure criterion	Present method (B_1)	Error $\left\|\frac{A-B_1}{A}\right\|$ %	Mindlin theory (B_2)	Error $\left\|\frac{A-B_2}{A}\right\|$ %
647·0	Polynomial maximum stress	654·11	1·1	716·20	10·7
	Tsai-Hill	658·85	1·8	721·23	11·5
	Hoffman	654·80	1·2	716·91	10·8
	Tsai-Wu	696·72	7·7	759·64	17·4
	Independent maximum stress	673·44	4·1	764·76	18·2

Table 5. Experimental and analytical first-ply failure loads of the $[0^\circ_8/90^\circ_8]_s$ plate

A. Experimental (N)	B. Analytical (N)				
	Failure criterion	Present method (B_1)	Error $\left\|\frac{A-B_1}{A}\right\|$ %	Mindlin theory (B_2)	Error $\left\|\frac{A-B_2}{A}\right\|$ %
2136·0	Polynomial maximum stress	2086·88	2·3	2391·98	12·0
	Tsai-Hill	2100·81	1·6	2405·44	12·6
	Hoffman	2088·85	2·2	2393·69	12·1
	Tsai-Wu	2207·07	3·3	2494·50	16·8
	Independent maximum stress	2200·83	3·0	2793·46	30·8

composite plates based on several phenomenological failure criteria. Experiments were performed to determine the actural first-ply failure loads of the plates. The comparison between the analytical and experimental results indicated that the present finite element coupled with phenomenological failure criteria are appropriate for the first-ply failure analysis of moderately thick laminated composite plates.

ACKNOWLEDGEMENT

This research was supported by the National Science Council of the Republic of China under Grant No. 83-0401-E-009-103. Their support is gratefully acknowledged.

REFERENCES

1. Turvey, G. J., An initial flexural failure analysis of symmetrically laminated cross-ply rectangular plates. *Int. J. Solids & Struct.*, **16** (1980) 451–63.
2. Turvey, G. J., Flexural failure analysis of angle-ply laminates of GFRP and CFRP. *J. Strain Anal.*, **15** (1980) 43–9.
3. Turvey, G. J., A study of the onset of flexural failure in cross-ply laminated strips. *Fibre Sci. Tech.*, **13** (1980) 325–36.
4. Turvey, G. J., Initial flexural failure of square, simply supported, angle-ply plates. *Fibre Sci. Tech.*, **15** (1981) 47–63.
5. Reddy, J. N. & Pandey, A. K., A first-ply failure analysis of composite laminates. *Computers & Struct.*, **25** (1987) 371–93.
6. Reddy, Y. S. N. & Reddy, J. N., Linear and nonlinear failure analysis of composite laminates with transverse shear. *Comp. Sci. Tech.*, **44** (1992) 227–55.
7. Kam, T. Y. & Lin, S. C., Reliability analysis of laminated composite plates. In *Proc. NSC, Part A*, **16** (1992) 163–71.
8. Kam, T. Y., Lin, S. C. & Hsiao, K. M., Reliability analysis of nonlinear laminated composite plate structures. *Comp. Struct.*, **25** (1993) 503–10.
9. T. Y. Kam & Sher, H. F., Nonlinear and first-ply failure analysis of laminated cross-ply plates. *J. Comp. Mat.*, **29** (1995) 463–82.
10. T. Y. Kam, Chang, R. R., Sher, H. F. & Chao, T. N., Prediction of first-ply failure strengths of laminated composite plates using a finite element approach. *Int. J. Solids & Struct.*, to appear (1995).
11. Jones, R. M., *Mechanics of Composite Materials*. Scripta Book Company, Washington, DC, 1975.
12. Pagano, N. J. & Hatfield, S. J., Elastic behavior of multilayered bidirectional composite. *AIAA J.*, **10** (1972) 931–3.
13. Reddy, J. N., A penalty plate-bending element for the analysis of laminated anisotropic composite plates. *Int. J. Num. Meth. Eng.*, **15** (1980) 1187–206.
14. S. C. Panda & R. Natarajan, Finite element analysis of laminated composite plate. *Int. J. Num. Meth. Engng*, **14** (1979) 69–79.
15. Mawenya, A. S. & Davies, J. D., Finite element bending analysis of multilayer plates. *Int. J. Num. Meth. Engng*, **8** (1974) 215–25.

16. Pagano, N. J., Exact solution for bidirectional composites and sandwich plates. *J. Comp. Mat.*, **4** (1970) 20–34.

17. Kam, T. Y. & Chang, R. R., Finite element analysis of shear deformable laminated composite plates. *J. Energy Resource Tech., ASME*, **115** (1993) 41–6.